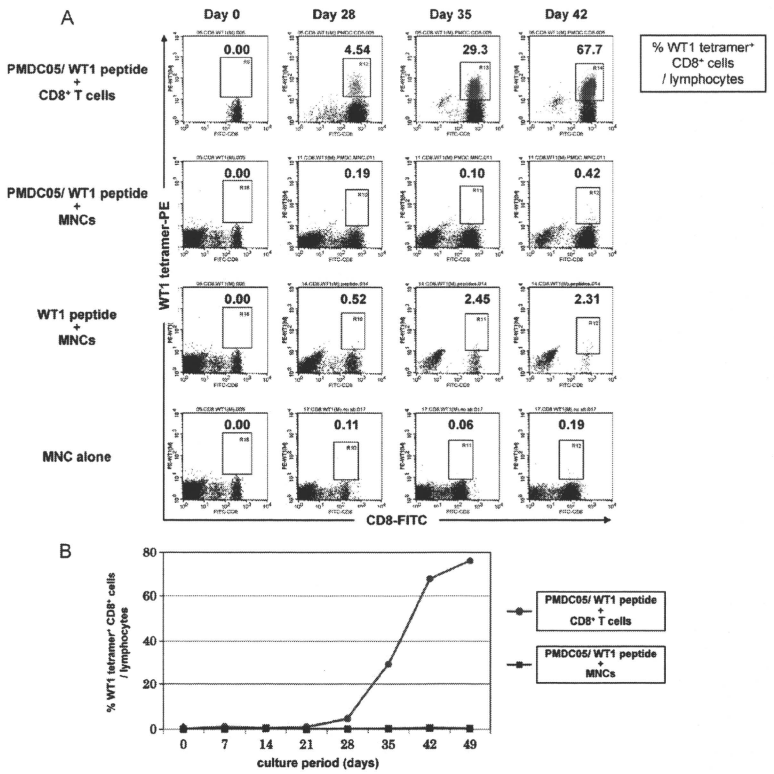

Fig. 5. Serial WT1 tetramer analysis of cultured cells consisting of WT1 peptide-pulsed PMDC05 and CD8+ T cells, WT1 peptide-pulsed PMDC05 and MNCs, MNCs with WT1 peptide and MNCs only. (A) Cultured cells in lymphocyte gate of FSC/SSC dot plots were displayed in the dot plots using CD8-FITC and WT1 tetramer-PE. Cells in gated area were calculated as percentage of WT1 tetramer+/CD8+ T cells among lymphocytes, which values were depicted above the gate. (B) A graph showing serial analysis for 49 days on percentages of WT1 tetramer+/CD8+ T cells among lymphocytes of co-cultures consisting of WT1 peptide-pulsed PMDC05 and CD8+ T cells or MNCs. These figures show representative data among three independent experiments.

efficiently in co-culture of normal PB CD8+ T cells with PMDC05 cells pulsed with tumor antigen (WT1 peptide) or viral antigen (CMVpp65 peptide). In the study using the WT1 peptide, although a high percentage of WT1 tetramer+/CD8+ T cells were generated in co-culture of CD8+ T cells with WT1 peptide-pulsed PMDC05, no WT1 tetramer+/CD8+ T cells were induced in co-culture of MNCs with WT1 peptide-pulsed PMDC05. The reason why no WT1 tetramer+/CD8+ T cells were observed in co-culture of MNCs with WT1 peptide-pulsed PMDC05 may be due to the usage of MNCs containing regulatory T cells, which might suppress the amplification of WT1 tetramer+/CD8+ T cells in the co-culture. On the contrary, in the study using CMVpp65 peptides, CMV tetramer+/CD8+ T cells were generated in co-culture of MNCs with CMV peptide-pulsed PMDC05, although the percentages of CMV tetramer+/CD8+ T cells generated from MNCs were less than those of CMV tetramer+/CD8+ T cells generated from CD8+ T cells. This data may suggest that CTL induction by viral antigens with high immunogenicity such as the CMVpp65 antigen are less influenced by the suppressive function of co-existing regulatory T cells compared with that by tumor antigens with low immunogenicity such as WT1 antigens. The present findings demonstrated that leukemic pDC line, PMDC05, with HLA-A*0201/2402 possesses a potent antigen presenting ability for generating tumor/viral antigen-specific CTLs in vitro.

The feasibility and safety of cellular immunotherapy using allogeneic dendritic cells have already been assessed in cancer clinical trials [27–29]. Trefzer et al. have reported that hybrid cell vaccines of autologous tumor cells fused with HLA matched allogeneic mDCs induced strong anti-tumor immune responses and clinical responses in melanoma patients [30]. Also, Rosenberg et al. have shown that in vitro expanded tumor infiltrating lymphocytes could be used in combination with vaccines and lymphodepletion for adoptive cell therapy in melanoma patients with good

Please cite this article in press as: Yamahira A, et al. Generation of antigen-specific cytotoxic T lymphocytes using a leukemic plasmacytoid dendritic cell line as antigen presenting cells. Leuk Res (2011), doi:10.1016/j.leukres.2010.12.003

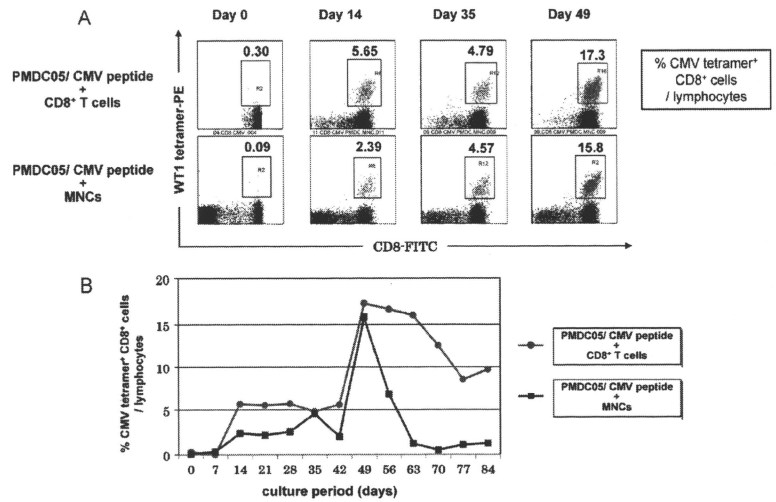

Fig. 6. Serial CMV tetramer analysis of cultured cells consisting of CMV peptide-pulsed PMDC05 and CD8+ T cells, and CMV peptide-pulsed PMDC05 and MNCs. (A) Cultured cells in lymphocyte gate of FSC/SSC dot plots were displayed in the dot plots using CD8-FITC and CMV tetramer-PE. Cells in gated area were calculated as percentage of CMV tetramer+/CD8+ T cells among lymphocytes, which values were depicted above the gate. (B) A graph showing serial analysis for 84 days on percentages of CMV tetramer+/CD8+ T cells among lymphocytes of co-cultures consisting of CMV peptide-pulsed PMDC05 and CD8+ T cells, and CMV peptide-pulsed PMDC05 and MNCs. These figures show representative data between two independent experiments.

response rates [31]. Recently mDCs pulsed with fusion antigen protein consisting of full-length prostatic acid phosphatase (PAP) and full-length GM-CSF were approved by U.S. Food and Drug Administration for the treatment of men with asymptomatic or minimally symptomatic metastatic, castrate resistant (hormone refractory) prostate cancer. The use of the mDC product prolonged overall survival among men enrolled in the Phase III clinical study compared with placebo group [32]. By contrast, prostate cancer immunotherapy using two allogeneic prostate cancer cell lines (PC3 and LNCaP), genetically modified through adenoviral transfer to secrete GM-CSF and irradiated to prevent further cell division, failed to show a survival benefit of this therapy in Phase III trials [33]. As demonstrated in Phase III trials of prostate cancer immunotherapy, mDC-based cellular immunotherapy is likely to be effective in cancer patients when the candidate is selected properly. Taken together with the above reports, our findings implied that PMDC05 could be applied for both adoptive transfer of antigen-specific CTLs and PMDC05-based DC active immunotherapy for patients with tumor or viral infection.

Conflict of interest

All authors have no conflict of interest to declare.

Contributors

AY, TN, NW and KK contributed to acquisition of data and analysis of data. MK and TT contributed to analysis and interpretation of data. SH, TF, KT and YA contributed to drafting and revising the article. MN and MT contributed to the conception and design of the study and drafting and revising the article.

References

[1] Dazzi F, Szydlo RM, Cross NC, et al. Durability of responses following donor lymphocyte infusions for patients who relapse after allogeneic stem cell transplantation for chronic myeloid leukemia. Blood 2000;96:2712–6.
[2] Yee C, Thompson JA, Byrd D, et al. Adoptive T cell therapy using antigen-specific CD8+ T cell clones for the treatment of patients with metastatic melanoma: in vivo persistence, migration, and antitumor effect of transferred T cells. Proc Natl Acad Sci USA 2002;99:16168–73.
[3] Bollard CM, Aguilar L, Straathof KC, et al. Cytotoxic T lymphocyte therapy for Epstein-Barr virus+ Hodgkin's disease. J Exp Med 2004;200:1623–33.
[4] Straathof KC, Bollard CM, Popat U, et al. Treatment of nasopharyngeal carcinoma with Epstein-Barr virus–specific T lymphocytes. Blood 2005;105:1898–904.
[5] Dudley ME, Wunderlich JR, Yang JC, et al. Adoptive cell transfer therapy following non-myeloablative but lymphodepleting chemotherapy for the treatment of patients with refractory metastatic melanoma. J Clin Oncol 2005;23:2346–57.
[6] Einsele H, Roosnek E, Rufer N, et al. Infusion of cytomegalovirus (CMV)-specific T cells for the treatment of CMV infection not responding to antiviral chemotherapy. Blood 2002;99:3916–22.
[7] Narita M, Watanabe N, Yamahira A, et al. A leukemic plasmacytoid dendritic cell line, PMDC05, with the ability to secrete IFN-alpha by stimulation via Toll-like receptors and present antigens to naive T cells. Leuk Res 2009;33:1224–32.
[8] Watanabe N, Narita M, Yamahira A, et al. Transformation of dendritic cells from plasmacytoid to myeloid in a leukemic plasmacytoid dendritic cell line (PMDC05). Leuk Res 2010;34:1517–24.
[9] Narita M, Kuroha T, Watanabe N, et al. Plasmacytoid dendritic cell leukemia with potent antigen-presenting ability. Acta Haematol 2008;120:91–9.
[10] Narita M, Takahashi M, Liu A, et al. Leukemia blast-induced T-cell anergy demonstrated by leukemia-derived dendritic cells in acute myelogenous leukemia. Exp Hematol 2001;29:709–19.
[11] Narita M, Tochiki N, Saitoh A, et al. Induction of antigen-specific cytotoxic T lymphocytes by using monocyte-derived DCs transfected with in vitro-transcribed WT1 or SART1 mRNA. Med Oncol 2009;26:429–36.
[12] Narita M, Masuko M, Kurasaki T, et al. WT1 peptide vaccination in combination with imatinib therapy for a patient with CML in the chronic phase. Int J Med Sci 2010;7:72–81.
[13] Furukawa T, Koike T, Ying W, et al. Establishment of a new cell line with the characteristics of a multipotential progenitor from a patient with chronic myelogenous leukemia in early erythroblastic crisis. Leukemia 1994;8:171–80.

Please cite this article in press as: Yamahira A, et al. Generation of antigen-specific cytotoxic T lymphocytes using a leukemic plasmacytoid dendritic cell line as antigen presenting cells. Leuk Res (2011), doi:10.1016/j.leukres.2010.12.003

[14] Irvine DJ, Doh J. Synthetic surfaces as artificial antigen presenting cells in the study of T cell receptor triggering and immunological synapse formation. Semin Immunol 2007;19:245–54.
[15] Koffeman E, Keogh E, Klein M, Prakken B, Albani S. Identification and manipulation of antigen specific T-cells with artificial antigen presenting cells. Methods Mol Med 2007;136:69–86.
[16] Rudolf D, Silberzahn T, Walter S, et al. Potent costimulation of human CD8 T cells by anti-4-1BB and anti-CD28 on synthetic artificial antigen presenting cells. Cancer Immunol Immunother 2008;57:175–83.
[17] Steenblock ER, Wrzesinski SH, Flavell RA, Fahmy TM. Antigen presentation on artificial acellular substrates: modular systems for flexible, adaptable immunotherapy. Expert Opin Biol Ther 2009;9:451–64.
[18] Cai Z, Brunmark A, Jackson MR, et al. Transfected Drosophila cells as a probe for defining the minimal requirements for stimulating unprimed CD8+ T cells. Proc Natl Acad Sci USA 1996;93:14736–41.
[19] Papanicolaou GA, Latouche JB, Tan C, et al. Rapid expansion of cytomegalovirus-specific cytotoxic T lymphocytes by artificial antigen-presenting cells expressing a single HLA allele. Blood 2003;102:2498–505.
[20] Hasan AN, Kollen WJ, Trivedi D, et al. A panel of artificial APCs expressing prevalent HLA alleles permits generation of cytotoxic T cells specific for both dominant and subdominant viral epitopes for adoptive therapy. J Immunol 2009;183:2837–50.
[21] Yuan J, Gallardo HF, Rasalan T, et al. In vitro expansion of Ag-specific T cells by HLA-A*0201-transfected K562 cells for immune monitoring. Cytotherapy 2006;8:498–508.
[22] Butler MO, Lee JS, Ansen S, et al. Long-lived antitumor CD8+ lymphocytes for adoptive therapy generated using an artificial antigen-presenting cell. Clin Cancer Res 2007;13:1857–67.
[23] Sasawatari S, Tadaki T, Isogai M, et al. Efficient priming and expansion of antigen-specific CD8+ T cells by a novel cell-based artificial APC. Immunol Cell Biol 2006;84:512–21.
[24] Chaperot L, Blum A, Manches O, et al. Virus or TLR agonists induce TRAIL-mediated cytotoxic activity of plasmacytoid dendritic cells. J Immunol 2006;176:248–55.
[25] Maeda T, Murata K, Fukushima T, et al. A novel plasmacytoid dendritic cell line, CAL-1, established from a patient with blastic natural killer cell lymphoma. Int J Hematol 2005;81:148–54.
[26] Aspord C, Charles J, Leccia MT, et al. A novel cancer vaccine strategy based on HLA-A*0201 matched allogeneic plasmacytoid dendritic cells. PLoS One 2010;5:e10458.
[27] Newton DA, Romano C, Gattoni-Celli S. Semiallogeneic cell hybrids as therapeutic vaccines for cancer. J Immunother 2000;23:246–54.
[28] Holtl L, Ramoner R, Zelle-Rieser C, et al. Allogeneic dendritic cell vaccination against metastatic renal cell carcinoma with or without cyclophosphamide. Cancer Immunol Immunother 2005;54:663–70.
[29] Hus I, Rolinski J, Tabarkiewicz J, et al. Allogeneic dendritic cells pulsed with tumor lysates or apoptotic bodies as immunotherapy for patients with early-stage B-cell chronic lymphocytic leukemia. Leukemia 2005;19:1621–7.
[30] Trefzer U, Herberth G, Wohlan K, et al. Tumour-dendritic hybrid cell vaccination for the treatment of patients with malignant melanoma: immunological effects and clinical results. Vaccine 2005;23:2367–73.
[31] Rosenberg SA, Dudley ME. Adoptive cell therapy for the treatment of patients with metastatic melanoma. Curr Opin Immunol 2009;21:233–40.
[32] Kantoff PW, Higano CS, Shore ND, et al. Sipuleucel-T immunotherapy for castration-resistant prostate cancer. N Engl J Med 2010;363:411–22.
[33] Higano C, Saad F, Somer B, et al. A phase III trial of GVAX immunotherapy for prostate cancer versus docetaxel plus prednisone in asymptomatic, castration-resistant prostate cancer (CRPC). J Clin Oncol 2009;LBA:150.

Please cite this article in press as: Yamahira A, et al. Generation of antigen-specific cytotoxic T lymphocytes using a leukemic plasmacytoid dendritic cell line as antigen presenting cells. Leuk Res (2011), doi:10.1016/j.leukres.2010.12.003

G Model
JCV-2131; No. of Pages 3
ARTICLE IN PRESS

Journal of Clinical Virology xxx (2010) xxx–xxx

Contents lists available at ScienceDirect

Journal of Clinical Virology

journal homepage: www.elsevier.com/locate/jcv

Short communication

Kinetics of Epstein-Barr virus load and virus-specific CD8+ T cells in acute infectious mononucleosis

Yo Hoshino[a], Kazuo Nishikawa[b], Yoshinori Ito[a], Kiyotaka Kuzushima[c], Hiroshi Kimura[d,*]

[a] Department of Pediatrics, Nagoya University Graduate School of Medicine, Japan
[b] Department of Pediatrics, Nagoya Ekisaikai Hospital, Japan
[c] Division of Immunology, Aichi Cancer Center Research Institute, Nagoya, Japan
[d] Department of Virology, Nagoya University Graduate School of Medicine, 65 Tsurumai-Cho, Showa-Ku, Nagoya 466-8550, Japan

ARTICLE INFO

Article history:
Received 20 October 2010
Received in revised form
24 November 2010
Accepted 25 November 2010

Keywords:
Epstein-Barr virus
Infectious mononucleosis
CTL
Viral load
EBV-specific CD8+ T cells

ABSTRACT

Background: During the convalescent phase of acute infectious mononucleosis (AIM), Epstein-Barr virus (EBV) load shrinks rapidly in association with a rapid decline in the number of EBV-specific CD8+ T cells. The actual contribution of EBV-specific CD8+ T cells in reducing EBV load, however, is not known.
Objectives: To clarify the impact of EBV-specific CD8+ T cells on the contraction of EBV load in AIM, we estimated half-lives of both EBV load and EBV-specific CD8+ T cells.
Study design: Blood was serially taken from five pediatric patients with AIM during the convalescent period, including the very early phase, and both EBV load and EBV-specific CD8+ T cell numbers were assayed.
Results: EBV load declined rapidly (half-life 1.5 d) during the first 2 weeks after onset of symptoms. This half-life was seven-fold shorter than that reported for CD27+ memory B cells. Subsequently, the EBV load declined much more slowly, with a half-life of 38.7 d. EBV-specific CD8+ T cell numbers also declined concomitantly with the decrease in EBV load. The half-life of EBV-specific CD8+ T cells during first 2 weeks was 2.9 d. The number of EBV-specific CD8+ T cells and the rate of change of viral load correlated significantly ($R^2 \geq 0.8$; $p \leq 0.02$).
Conclusions: The short half-life of EBV load, together with the strong correlation between the number of EBV-specific CD8+ T cells and the rate of change of viral load indicates an active role for EBV-specific CD8+ T cells in elimination of EBV in AIM.

1. Background

Epstein-Barr virus (EBV) is a ubiquitous viral pathogen that causes acute infectious mononucleosis (AIM) and various malignant diseases, such as Burkitt's lymphoma, nasal NK/T lymphoma, nasopharyngeal carcinoma, and post-transplant lymphoproliferative disorders, in both immunocompromised and immunocompetent hosts.[1] EBV-specific CD8+ T cells play important roles in the control of EBV in these diseases.[2] During the convalescent phase of AIM, the EBV load shrinks rapidly in association with a rapid decline in the number of EBV-specific CD8+ T cells, itself caused by activation-induced cell death.[3] However, the extent to which EBV-specific CD8+ T cells contribute to the decline in EBV load in peripheral blood mononuclear cells remains unknown.

2. Objectives

To clarify the impact of EBV-specific CD8+ T cells on the decline in EBV load, we estimated the half-lives of EBV load and EBV-specific CD8+ T cells during the convalescent period of AIM and also evaluated the correlation between them.

3. Study design

Blood samples were serially obtained from five pediatric patients with AIM after written informed consent had been obtained from their parents. AIM was diagnosed by clinical findings and serological examinations, as previously described.[4] Their ages ranged from 5 to 14 years (median, 9 years). The first samples were obtained within the first week of onset of AIM symptoms. Peripheral blood mononuclear cells were separated, frozen, and stored until required. EBV load in peripheral blood mononuclear cells was measured by real-time PCR and expressed as copies/microgram DNA.[4,5] EBV-specific CD8+ T cells were enumerated by intracellular interferon-γ assay against autologous lymphoblastoid cell lines by

Abbreviations: EBV, Epstein-Barr virus; AIM, acute infectious mononucleosis.

* Corresponding author. Tel.: +81 52 744 2207; fax: +81 52 744 2452.
E-mail address: hkimura@med.nagoya-u.ac.jp (H. Kimura).

1386-6532/$ – see front matter © 2010 Elsevier B.V. All rights reserved.
doi:10.1016/j.jcv.2010.11.017

Please cite this article in press as: Hoshino Y, et al. Kinetics of Epstein-Barr virus load and virus-specific CD8+ T cells in acute infectious mononucleosis. *J Clin Virol* (2011), doi:10.1016/j.jcv.2010.11.017

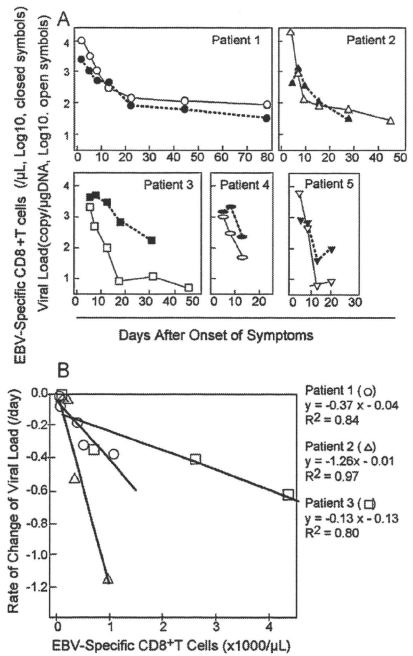

Fig. 1. Kinetics of Epstein-Barr virus (EBV) load and EBV-specific $CD8^+$ T cells in patients with acute infectious mononucleosis. (A) EBV vial load was measured by real-time PCR (open symbols connected with solid lines), and EBV-specific $CD8^+$ T cell counts by intracellular interferon-γ assay against autologous lymphoblastoid cell lines and flow cytometry (closed symbols connected with broken lines). (B) Correlation between EBV-specific $CD8^+$ T cell counts and rate of change in EBV load was estimated by linear regression analysis. Approximations of the rate of change were calculated from three data points. Using v_1, v_2, and v_3, which are the natural logarithms of viral loads at t_1, t_2, and t_3, respectively, the following equation was used to calculate the rate of change of viral load for a unit of viral load at $t = t_2$: $dv/dt_{(t=t2)} = (x_2 - x_1)(t_3 - t_2)/(t_2 - t_1)/(t_3 - t_1) + (x_3 - x_2)(t_2 - t_1)/(t_3 - t_2)/(t_3 - t_1)$. Solid lines indicate linear regression curves for patients 1, 2, and 3, from whom sufficient data points were obtained.

flow cytometry.[3,6]

4. Results

First, we analyzed the kinetics of EBV load and number of EBV-specific $CD8^+$ T cells. EBV load was highest at the time of first sampling (2–6 d after onset) in all patients and decreased thereafter (Fig. 1A). Peak viral loads were $10^{4.1}$, $10^{4.3}$, $10^{3.3}$, $10^{3.0}$, and $10^{3.8}$ per μg DNA in patients 1, 2, 3, 4, and 5, respectively. EBV viral loads declined rapidly during the first 1–2 weeks after onset and more slowly thereafter (Fig. 1A). The mean estimated half-life of EBV load during the early convalescent period (~2 weeks after onset) was 1.5 ± 0.2 d (Table 1); this is seven-fold shorter than that reported for $CD27^+$ memory B cells (11.1 d).[7] EBV infection in the peripheral blood of AIM patients is restricted to $CD27^+$ memory B cells.[8] The mean estimated half-life of EBV load after the 2 weeks was 38.7 ± 15.0. In contrast, number of EBV-specific $CD8^+$ T cells increased slightly in three of the five patients and then declined (Fig. 1A). In the remaining patients, the number of EBV-specific $CD8^+$ T cells peaked at the time of their first visit ($10^{3.5}$ and $10^{2.9}$ per μL blood in patients 1 and 5, respectively). Number of EBV-specific $CD8^+$ T cells declined almost parallel with viral load (half-life 2.9 ± 0.4 d) during the early convalescent period (Table 1).

Table 1
Half-lives of Epstein-Barr virus (EBV) load and EBV-specific $CD8^+$ T cells in patients with acute infectious mononucleosis.

Patient	Half-life of EBV load (days)		Half-life of EBV-specific $CD8^+$ T cells in acute phase (days) (within 2 weeks of onset)
	Acute phase (within 2 weeks of onset)	Convalescent phase (after 2 weeks of onset)	
1	2.2	22.6	3.8
2	1.5	24.9	2.9
3	1.6	68.7	3.8
4	1.6	n.a.	2.5
5	0.7	n.a.	1.6
Mean ± SE	1.5 ± 0.2	38.7 ± 15.0	2.9 ± 0.4

The shorter half-life of EBV load compared with normal memory B cells suggests the presence of a mechanism that actively removes EBV from blood, such as cytotoxic immune effecter cells. We hypothesized that EBV-specific $CD8^+$ T cells play an important role in clearing EBV from blood. EBV load may decrease at a rate proportional to the number of EBV-specific $CD8^+$ T cells. To prove this hypothesis, we transformed the time-series of EBV load data into rate of change and examined the correlation between the number of EBV-specific $CD8^+$ T cells and the rate of change in viral load. Because multiple data points were necessary for regression analysis, three of the five patients (1, 2, and 3) were analyzed. As shown in Fig. 1B, the analysis revealed a significant positive linear correlation between the rate of change in viral load and the number of EBV-specific $CD8^+$ T cells ($R^2 \geq 0.8$, $p \leq 0.02$).

5. Discussion

To clarify the impact of EBV-specific $CD8^+$ T cells on the decline in EBV load, we estimated the half-lives of both EBV load and EBV-specific $CD8^+$ T cells during the very early phase of the convalescent period of AIM using intervals as short as 2 d. We also evaluated the correlation between the EBV load and the number of EBV-specific $CD8^+$ T cells. Our data indicate that during the very early period of AIM, the half-life of EBV load is shorter than that of normal memory B cells and that the rate of change in EBV load was correlated with the number of EBV-specific $CD8^+$ T cells in a linear manner. These results suggest that EBV-specific $CD8^+$ T cells actively contribute to the decline in EBV load.

Recently, Hadinoto *et al.* reported that linear exponential decay of latent EBV load with a half-life of 7.5 ± 3.7 d was found in patients with AIM during the 30–50 d after the first clinic visit.[9] Due to its similarity to the reported half-life of memory B cells (11.1 d),[7] the authors proposed a model of exponential decay of EBV-infected cells by simple homeostasis of memory B cells, suggesting a passive role for cell-mediated immunity. Hadinoto's paper did not specify the interval between the onset of symptoms and the first clinic visit, and the intervals between assays seemed to be around 1 week. It is possible that EBV-specific $CD8^+$ T cells play an important role in the control of EBV load during an earlier stage of AIM. In the very early phase of AIM, EBV infects naïve B cells that express full sets of latent EBV genes.[2] These naïve B cells are either eliminated by EBV-specific CTL or differentiate into memory B cells. In the second phase, the EBV-infected memory B cells express only

Please cite this article in press as: Hoshino Y, et al. Kinetics of Epstein-Barr virus load and virus-specific $CD8^+$ T cells in acute infectious mononucleosis. *J Clin Virol* (2011), doi:10.1016/j.jcv.2010.11.017

restricted kinds of EBV genes,[2] which may help with evasion from EBV-specific CD8+ cells. In the present study, we obtained 2–3 samples per week from the very early period of acute-phase AIM. Thus, the more frequent samples taken at an earlier stage of disease may be the reason for the disagreement in EBV load half-life. In fact, if samples are taken only once per week, a half-life shorter than 3 days will not be detected in two weeks or less.

During the acute phase of AIM, viral loads decreased, even in blood taken only 2 d after symptom onset. Interestingly, we observed a transient increase in EBV-specific CD8+ T cells in three patients; this may be due to a programmed proliferation of T cells.[10–12] In studies in mice, the decrease in pathogen-specific CD8+ T cells is programmed and independent of antigen loads (programmed contraction).[13,14] This is in agreement with current concepts of antigen-driven expansion and contraction of CD8+ T cells during acute infection.[3] A recent paper proposed the model of EBV dynamics in post-transplant lymphoproliferative disorders.[15] The model estimates both doubling times and half-lives of EBV in various situations under the antiviral agents, Rituximab, or adoptive immunotherapy with or without taking into account episomal or lytic origins.

In conclusion, the shorter half-life of EBV load together with the strong correlation between EBV-specific CD8+ T cell numbers and the rate of change of viral load suggests an active role for EBV-specific CD8+ T cells in the elimination of EBV. Further investigations of the interaction between EBV and EBV-specific CD8+ T cells during the period of increasing viral load will be necessary to understand the dynamic interaction between EBV and the immune system during AIM.

Conflict of interest statement

All authors state that they have no conflicts of interest that could inappropriately influence this work.

Acknowledgements

We thank Drs. Jeffrey I. Cohen and Kennichi C. Dowdell at Laboratory of Clinical Infectious Diseases, NIAID, for advice and suggestions. This study was supported by a grant from the Ministry of Education, Culture, Sports, Science and Technology of Japan (13670793).

References

1. Cohen JI. Epstein-Barr virus infection. *N Engl J Med* 2000;**343**(7):481–92.
2. Hislop AD, Taylor GS, Sauce D, Rickinson AB. Cellular responses to viral infection in humans: lessons from Epstein-Barr virus. *Annu Rev Immunol* 2007;**25**:587–617.
3. Hoshino Y, Morishima T, Kimura H, Nishikawa K, Tsurumi T, Kuzushima K. Antigen-driven expansion and contraction of CD8+-activated T cells in primary EBV infection. *J Immunol* 1999;**163**(10):5735–40.
4. Kimura H, Morita M, Yabuta Y, Kuzushima K, Kato K, Kojima S, et al. Quantitative analysis of Epstein-Barr virus load by using a real-time PCR assay. *J Clin Microbiol* 1999;**37**(1):132–6.
5. Hoshino Y, Kimura H, Tanaka N, Tsuge I, Kudo K, Horibe K, et al. Prospective monitoring of the Epstein-Barr virus DNA by a real-time quantitative polymerase chain reaction after allogenic stem cell transplantation. *Br J Haematol* 2001;**115**(1):105–11.
6. Kuzushima K, Kimura H, Hoshino Y, Yoshimi A, Tsuge I, Horibe K, et al. Longitudinal dynamics of Epstein-Barr virus-specific cytotoxic T lymphocytes during posttransplant lymphoproliferative disorder. *J Infect Dis* 2000;**182**(3):937–40.
7. Macallan DC, Wallace DL, Zhang Y, Ghattas H, Asquith B, de Lara C, et al. B-cell kinetics in humans: rapid turnover of peripheral blood memory cells. *Blood* 2005;**105**(9):3633–40.
8. Hochberg D, Souza T, Catalina M, Sullivan JL, Luzuriaga K, Thorley-Lawson DA. Acute infection with Epstein-Barr virus targets and overwhelms the peripheral memory B-cell compartment with resting: latently infected cells. *J Virol* 2004;**78**(10):5194–204.
9. Hadinoto V, Shapiro M, Greenough TC, Sullivan JL, Luzuriaga K, Thorley-Lawson DA. On the dynamics of acute EBV infection and the pathogenesis of infectious mononucleosis. *Blood* 2008;**111**(3):1420–7.
10. Kaech SM, Ahmed R. Memory CD8+ T cell differentiation: initial antigen encounter triggers a developmental program in naive cells. *Nat Immunol* 2001;**2**(5):415–22.
11. van Stipdonk MJ, Lemmens EE, Schoenberger SP. Naive CTLs require a single brief period of antigenic stimulation for clonal expansion and differentiation. *Nat Immunol* 2001;**2**(5):423–9.
12. van Stipdonk MJ, Hardenberg G, Bijker MS, Lemmens EE, Droin NM, Green DR, et al. Dynamic programming of CD8+ T lymphocyte responses. *Nat Immunol* 2003;**4**(4):361–5.
13. Badovinac VP, Porter BB, Harty JT. Programmed contraction of CD8(+) T cells after infection. *Nat Immunol* 2002;**3**(7):619–26.
14. Badovinac VP, Harty JT. Programming, demarcating, and manipulating CD8+ T-cell memory. *Immunol Rev* 2006;**211**:67–80.
15. Funk GA, Gosert R, Hirsch HH. Viral dynamics in transplant patients: implications for disease. *Lancet Infect Dis* 2007;**7**(7):460–72.

Please cite this article in press as: Hoshino Y, et al. Kinetics of Epstein-Barr virus load and virus-specific CD8+ T cells in acute infectious mononucleosis. *J Clin Virol* (2011), doi:10.1016/j.jcv.2010.11.017

Int J Hematol
DOI 10.1007/s12185-010-0758-7

ORIGINAL ARTICLE

Activation of T-cell receptor signaling in peripheral T-cell lymphoma cells plays an important role in the development of lymphoma-associated hemophagocytosis

Jun An · Hiroshi Fujiwara · Koichiro Suemori · Toshiyuki Niiya · Taichi Azuma · Kazushi Tanimoto · Toshiki Ochi · Yoshiki Akatsuka · Junichi Mineno · Hidetoshi Ozawa · Fumihiko Ishikawa · Kiyotaka Kuzushima · Masaki Yasukawa

Received: 15 October 2010 / Revised: 14 November 2010 / Accepted: 17 December 2010

Abstract Peripheral T-cell lymphoma (PTCL) is a biologically diverse lymphoid malignancy. The clinical aggressiveness associated with hemophagocytic syndrome (HS) is a characteristic of PTCL, being more distinctive in $CD8^+$ PTCL. However, the underlying mechanism of PTCL-associated HS has not yet been fully investigated. We newly established a novel IL-2-dependent $CD8^+$ PTCL lymphoma cell line (T8ML-1) from a patient with $CD8^+$ PTCL who suffered recurrent HS accompanying disease flare-up. Focusing on the lymphoma cell T-cell receptor (TCR), we examined the lymphoma cell functions responsible for such clinical manifestations. First, T8ML-1.1 in which endogenous TCR-α/β chains were silenced by siRNAs, and T8ML-1.2 in which endogenous TCR-α/β chains were replaced with HLA-A*24:02-restricted and $WT1_{235-243}$-specific TCR-α/β, were established. T8ML-1 exerted phytohemagglutinin (PHA)-dependent cytotoxicity via granular exocytosis. Additionally, soluble factors produced by PHA-stimulated T8ML-1, which included INF-γ and TNF-α, but not by simple-cultured T8ML-1, caused human monocytes to exhibit erythrophagocytosis and thrombophagocytosis in vitro. PHA binding induced phosphorylation of CD3ζ chain. Furthermore, both cytotoxicity and hemophagocytosis were completely inhibited by T8ML-1.1, but eventually restored by T8ML-1.2. These data suggest that exogenous activation of TCR signaling in PTCL cells might play an important role in the formation of PTCL-associated HS.

Keywords Peripheral T-cell lymphoma · Lymphoma-associated hemophagocytic syndrome · T-cell receptor signaling

J. An · H. Fujiwara (✉) · K. Suemori · T. Azuma · K. Tanimoto · T. Ochi · M. Yasukawa
Department of Bioregulatory Medicine, Graduate School of Medicine, Ehime University, Toon, Ehime, Japan
e-mail: yunarief@m.ehime-u.ac.jp

H. Fujiwara · M. Yasukawa
Department of Cell Growth and Cancer Regulation, Ehime University Proteomedicine Research Center, Shitsukawa, Toon, Ehime 791-0295, Japan

T. Niiya
Division of Clinical Laboratory, Ehime University Hospital, Toon, Japan

Y. Akatsuka · K. Kuzushima
Aichi Cancer Center, Nagoya, Aichi, Japan

Y. Akatsuka
Department of Hematology, Fujita Health University, Toyoake, Aichi, Japan

J. Mineno
Takara Bio Inc., Ohtsu, Shiga, Japan

H. Ozawa · F. Ishikawa
Research Unit for Human Disease Models, RIKEN Research Center for Allergy and Immunology, Yokohama, Kanagawa, Japan

1 Introduction

Peripheral T-cell lymphoma (PTCL) is a biologically diverse lymphoid malignancy [1]. Most cases of PTCL are $CD4^+$ [2], and disease aggressiveness is more pronounced in $CD8^+$ PTCL [3]. Patients with PTCL,NOS (PTCL not otherwise specified), which is the most common subtype of PTCL, frequently display advanced disease with the involvement of systemic organs, such as the liver, spleen, bone marrow, and even peripheral blood [4]. In terms of biological background,

Published online: 13 January 2011

it has been revealed that PTCL,NOS lymphoma cells show pathological features and a gene expression pattern similar to those of activated peripheral T-cells [5].

Lymphoma-associated hemophagocytic syndrome (LAHS), characterized by persistent fever, hepatosplenomegaly and severe peripheral pancytopenia is a common and often life-threatening complication of PTCL [6–8]. As to the causative mechanism of LAHS, the role of multiple proinflammatory cytokines that activate non-malignant macrophages that are overproduced in PTCL has been emphasized [6–10], among which interferon (IFN)-γ and tumor necrosis factor (TNF)-α are representative [11–13]; however, details remain undetermined.

On the other hand, the activation status of T-cell receptor (TCR) signaling of lymphoma cells has recently become a focus of attention [14, 15], in terms of the prognostic value [16–19], the therapeutic target [5, 20, 21], and the tumorigenesis of PTCL [22, 23].

In the present study, we newly established a $CD8^+$ PTCL cell line from a patient with PTCL who characteristically displayed refractory LAHS and multiple organ failure. Then focusing on the TCR signaling, using this cell line and genetically modified subclones, we examined the functional features of $CD8^+$ PTCL cells that are responsible for tissue destruction and LAHS, and consequently, were able to demonstrate a close correlation between TCR signaling and the development of LAHS.

2 Patient and methods

2.1 Patient history

A 64-year-old female patient with PTCL,NOS demonstrating systemic lymphadenopathy was referred to our university hospital at the beginning of 2007. Patient lymphoma cells were positive for surface CD3, CD8, CD30, HLA-DR, TCR-α/β, and intracellular granzyme B, but negative for surface CD4, CD25, TCR-γ/δ, cytoplasmic anaplastic lymphoma kinase (ALK), and Epstein–Barr virus (EBV)-encoded small RNAs (EBER 1/2) by in situ hybridization and monoclonal integration of EBV by Southern blotting. Despite multiple courses of combination chemotherapies, the patient died due to progression of the disease in 2 years. This patient characteristically demonstrated recurrence of severe pancytopenia due to bone marrow involvement of LAHS and multiple organ dysfunction, which coincided with the flare-up of the PTCL. Permission for autopsy was not granted by the family members.

2.2 Cell lines and primary cells

Jurkat, K562, HLA-A*24:02 transduced K562 (K562-A24), and HLA-A*24:02 transduced C1R (C1R-A24) cells were ordinarily cultured in RPMI 1640 with 10% FCS (Invitrogen GIBCONY), penicillin (100 U/ml), and streptomycin (100 mg/ml) (complete culture medium, CM). The patient's lymphoma cells were obtained from a biopsied morbid lymph node, and peripheral blood mononuclear cells (PBMC) were also obtained from healthy volunteers, given written informed consents with the Declaration of Helsinki. Approval for the use of the patient's samples was obtained from the institutional review board of Ehime University Hospital.

2.3 Establishment of a novel $CD8^+$ peripheral T-cell lymphoma cell line: T8ML-1

Patient's $CD3^+/CD8^+$ lymphoma cells were cultured in CM with 10 U/ml recombinant human IL-2 (Roche Diagnostics GmbH, Mannheim, Germany), and eventually, a novel $CD8^+$ T-cell lymphoma cell line, designated T8ML-1, was established.

2.4 Generation of a T8ML-1 subclone in which endogenous TCR was knocked down using shRNA: T8ML-1.1

Full-length endogenous TCR-α/β chains of T8ML-1 were determined by the multiplex PCR method as described elsewhere [24]. Briefly, total RNA was prepared from T8ML-1 and cDNA was synthesized. All primers for TCR-Vβ, TCRCβ, TCR-Vα and TCRCα were described previously [24]. Reverse transcription polymerase chain reaction (RT-PCR) conditions for TCR-Vβ were: 95°C for 9 min, 30 cycles of 94°C for 30 s, 58°C for 20 s, 72°C for 30 s, and finally one cycle of 72°C for 10 min. RT-PCR conditions for TCR-Vα: for both first PCR with the 3′-outer primer and nested PCR with the inner 3′-primer were: one cycle of 95°C for 10 min, followed by 35 cycles of 94°C for 30 s, 50°C for 15 s, 72°C for 30 s, and finally one cycle of 72°C for 10 min. Both TCR-Vα and β PCR products were directly sequenced using an ABI PRISM 3700 sequencer (Applied Biosystems, Foster City, CA). The determined endogenous TCR-α and -β chains of T8ML-1 were Vα12.2/J6/Cα, and Vβ15.1/J2.1/Cβ2, respectively, using human TCR gene database (http://imgt.cines.fr/) and international ImMunoGeneTics database (IMGT) [25].

Each siRNA for endogenous Vα12.2 (5′-CCAAT GGTGACAAAGAAGA-3′) and Vβ15.1 (5′-GATACCA GGTTACCCAGTT-3′) of T8ML-1 was synthesized into double-stranded DNA (shDNA) and cloned into the pSINsi-DK vector (Takara code 3664) (Takara Bio Inc., Ohtsu, Japan). shRNA for Vα was driven by the human U6 promoter and that for Vβ was driven by the murine U6 promoter. shRNAs for each TCR-α/β genes were transduced into T8ML-1 with a bicistronic pSINsi-DK retroviral vector in

two step method reported previously [26]. Briefly, the shRNAs for the endogenous TCRs of T8ML-1 were transduced into T8ML-1 by VSVG-pseudotyped retrovirus infection on RetroNectin (Takara Bio, Ohtsu, Japan)-coated plates. Transfectants lacking surface TCR-$\alpha\beta$ were sorted using FACS Aria (Becton–Dickinson, Foster City, CA) and then cultured in CM with IL-2 and 500 μg/ml neomycin (Invitrogen GIBCO, NY). Finally, T8ML-1.1: the subclone of T8ML-1 in which endogenous TCR-α/β genes had been stably knocked out was obtained. Bulk subset of T8ML-1 of which endogenous TCR-α/β genes had been partially knocked out was also obtained and designated T8ML-1.1v.

2.5 Re-introduction of WT1-specific TCR-α/β genes into T8ML-1.1: T8ML-1.2

Full-length TCR-α/β genes obtained from a HLA-A*2402-restricted WT1 (WT1aa 235–243: CMTWNQMNL)-specific CTL clone (Vα20/J33/Cα for TCR-α and Vβ5.1/J2.1/Cβ2 for TCR-β, respectively) [27] was bicistronic-lentivirally transduced into T8ML-1.1 to replace the endogenous TCR-α/β with predetermined TCR-α/β, as described above. The WT1-specific TCR-α/β gene transduced T8ML-1.1 was designated T8ML-1.2. Stable expression of the transduced WT1-specific TCR-α/β was genetically analyzed by RT-PCR for both transduced Vβ 5.1 and Vα20 mRNAs (data not shown).

2.6 Flow cytometry assay

The surface and cytoplasmic antigens of cells from patient, T8Ml-1, T8ML-1.1, and T8ML-1.2, and monocytes isolated from PBMCs from the healthy volunteer were detected by a FACSCalibur and analyzed using Cell Quest (Becton Dickinson, Foster City, CA) and FlowJo (TreeStar) software. Anti-CD3, anti-CD4, anti-CD8, anti-CD11b, anti-CD14, anti-CD25, anti-CD49a, anti-CD56, and anti-CD69 monoclonal antibodies (mAb) conjugated with FITC, PE, APC (BD Bioscience, San Jose, CA), PE-or FITC-conjugated anti-human Vβ5.1 mAb (Immunotech, Marseille, France), FITC-conjugated anti-human TCR-$\alpha\beta$, and CD30 mAb (BioLegend, San Diego, CA) and PE-conjugated anti-human Fas and Fas-Ligand mAb (MBL, Woburn, MA), were used as cell-surface markers. PE-conjugated anti-human granzyme B mAb (R&D Systems, Minneapolis, MN) and FITC-conjugated anti-human perforin (BioLegend, San Diego, CA) were used for cytoplasmic staining.

2.7 Cytotoxicity assay

Phytohemagglutinin (PHA)-dependent cytotoxicity [28] of T8ML-1 was examined by standard 4 h culture ^{51}chromium release assay as described elsewhere [29]. Briefly, 1×10^4 ^{51}Cr ($Na_2{}^{51}CrO_4$) (New England Nuclear, Boston, MA)-labeled Jurkat and K562 cells (as target cells) were co-cultured with various numbers of T8ML-1 cells (as effector cells) with 1 μg/ml PHA-P (Sigma-Aldrich) in 96-well plates. The percentage of specific lysis was calculated using the formula: [(experimental release (cpm) − spontaneous release (cpm))/(maximal release (cpm) − spontaneous release (cpm))] × 100 (%). For inhibition assay, various concentrations of anti-Fas monoclonal antibody (MBL), or concanamycin A (ConA) (Wako Pure Chemical Industries, Osaka, Japan), were used. All experiments were performed in triplicate.

2.8 Enzyme-linked immunosorbent assay

Supernatants of PHA-P-treated T8ML-1, T8ML-1.1, and T8ML-1.2, were determined for IFN-γ and TNF-α by a commercial ELISA kit (R&D Systems).

2.9 Western blotting analysis

Phosphorylation of the CD3ζ chain was examined by Western blotting as described elsewhere [30]. Briefly, cell lysates from 1×10^6 T8ML-1, T8ML-1.1, T8ML-1.2 cells and normal CD8$^+$ T-lymphocytes treated for 24 h with PHA-P or anti-CD3 moAb (OKT-3) (BioLegend) were collected. After electrophoresis in 12.5% SDS–polyacrylamide gel, blots were reacted with anti-human CD3-ζ mouse moAb (BD Biosciences) and visualized using an enhanced chemiluminescence system (GE Healthcare UK Ltd. Buckinghamshire). Anti-β-actin mouse moAb (Sigma-Aldrich) was used for control. Representative data from 3 experiments are shown.

2.10 Phagocytosis assay

Phagocytosis of CD14-positive human monocytes selected from healthy volunteer PBMC (Milteny Biotec, Auburn, CA) (1×10^6/ml), which were incubated for 24 h with culture supernatants from T8ML-1, T8ML-1.1 and T8ML-1.2 treated or untreated with PHA-P for 24 h was examined by IgG-FITC-conjugated latex beads in accordance with manufacturer's instructions (Cayman Chemical Company, Ann Arbor, MI). FITC-positive monocytes that engulfed FITC-labeled latex beads were detected by flow cytometry. Fluorescence Index (FI) was calculated by the formula: [(mean fluorescence intensity (MFI) of monocytes co-cultured in PHA-P-treated supernatant − MFI of monocytes co-cultured in PHA-P-untreated supernatant)/MFI of monocytes co-cultured in PHA-P-untreated supernatant].

2.11 Hemophagocytosis assay

Hemophagocytosis caused by monocytes that had been cultured in supernatants from PHA-P-treated or untreated T8ML-1, and T8ML-1.1 was examined. Red blood cells

(RBC), platelets (PLT), and monocytes were obtained from the same donor by Ficoll–Hypaque centrifugation technique for RBC and monocytes, and by the ordinary plateletpheresis method for PLT. One million monocytes were co-cultured for 24 h with 1×10^6 RBC or 1×10^3 PLT in 1 ml of culture supernatant from PHA-P-treated or untreated T8ML-1, and T8ML-1.1, respectively. Cytospin specimens of harvested monocytes were stained with May-Giemsa, and examined microscopically. Representative micrographs from 3 experiments are shown.

2.12 Statistical analysis

The paired t test was used to assess the statistical significance of differences at a p value of <0.05.

3 Results

3.1 Characterization of a novel IL-2 dependent $CD8^+$ PTCL cell line: T8ML-1

Both the primary lymphoma cells (Fig. 1a lt.) and T8ML-1 (Fig. 1a rt.) were granular lymphocytes. T8ML-1 displayed a complex chromosomal abnormality, and negative for monoclonal integration of the EBV genome. In addition, T8ML-1 was genetically shown to be identical to primary lymphoma cell by TCR-β gene rearrangement analysis (data not shown). The cell-surface phenotypes of the primary lymphoma cells and T8ML-1 are compared in Table 1. The expression of surface IL-2 receptor α (CD25) was augmented in T8ML-1, whose growth was dependent on a low dose of IL-2. In the absence of IL-2, activation with both PHA-P and OKT-3 could transiently prolong the survival of T8ML-1 (data not shown).

3.2 Lectin-dependent cytotoxicity of T8ML-1 via cytotoxic granular exocytosis

In order to examine the features of T8ML-1, responsible for recurrence of multiple organ damage coincident with flare-up of the lymphoma in this patient, we first examined the lectin-dependent cytotoxicity. We found that T8ML-1 non-epitope-specifically exerted PHA-P-dependent cytotoxicity against both Jurkat and K562 cells (Fig. 2a). Cytotoxicity against both targets was significantly inhibited by ConA, an inhibitor of the perforin/granzyme B pathway, in a dose-dependent manner (Fig. 2b), but not by anti-Fas antibody (data not shown). Positive expression of both intracytoplasmic perforin and granzyme B was further confirmed by flow cytometry (Fig. 2c).

Table 1 Immunophenotype of primary lymphoma cell and T8ML-1

Markers	Positive cells (%)	
	Primary cells	T8ML-1
CD2	97.8	99.9
CD3	95.2	99.9
CD4	15.5	0
CD5	32.2	0
CD7	23.7	0.27
CD8	80.4	99.9
CD10	5.2	0.3
CD16	1.4	n.d.
CD19	0.6	n.d.
CD20	5.6	0.1
CD21	5.6	0.1
CD23	0.3	0
CD25	3.3	72.5
CD30	98.6	98.9
CD38	n.d.	54.3
CD56	1.4	0.1
HLA-DR	93.8	99.8
sImg-κ	0.4	0
sImg-λ	0.8	0
TCR-$\alpha\beta$	95.6	99.2
TCR-$\gamma\delta$	0.1	0

sImg surface immunoglobulin, *n.d.* not done

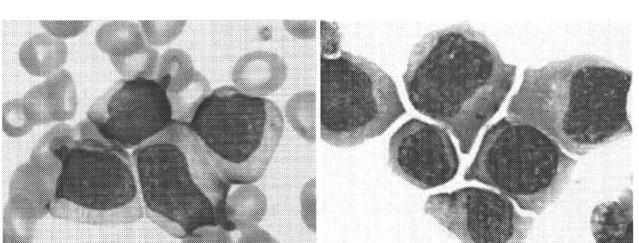

Fig. 1 Morphology. Morphology of the patient's lymphoma cells (*left*) and T8ML1 cells (*right*) stained with May-Giemsa. (×100)

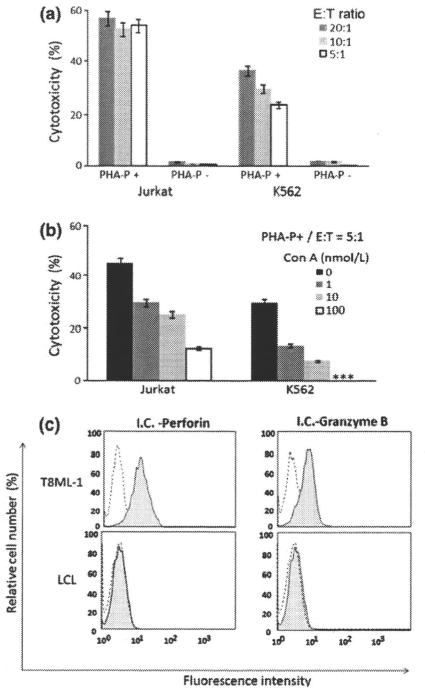

Fig. 2 **a** Lectin-dependent cytotoxicity of T8ML-1 against Jurkat and K562 measured by standard ^{51}Cr-release assay. Data are shown as mean ± standard deviation (SD) from three independent experiments. *PHA-P* phytohemagglutinin-P, *E:T ratio* effector-to-target cell ratio. **b** Concanamycin A (ConA) inhibited T8ML-1-mediated lectin-dependent cytotoxicity. Lectin-dependent cytotoxicity by T8ML-1 against both Jurkat and K562 was dose-dependently inhibited by ConA. Experiments were performed at an *E:T* ratio of 5:1 in triplicate. Data are shown as mean ± SD. ***less than detectable. **c** Clear intracellular expression of perforin and granzyme B in T8ML-1. LCL:EBV-immortalized human B cell line as a negative control. *I.C.* intracytoplasmic

3.3 Lectin-dependent cytotoxicity of T8ML-1 requires the cell-surface TCR molecule

Next we examined the involvement of the TCR molecule in this lectin-dependent cytotoxicity of T8ML-1. Initially we observed a positive correlation between this lectin-dependent cytotoxicity and the surface expression level of TCR-α/β and CD3. As shown in Fig. 3a, the lectin-dependent cytotoxicity of T8ML-1 against Jurkat cells with full expression of the surface TCR-α/β and CD3 molecules was

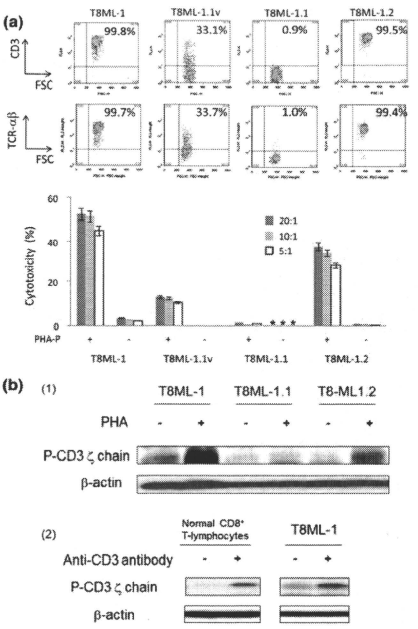

Fig. 3 **a** Close correlation between lectin-dependent cytotoxicity and the cell-surface expression level of TCR/CD3 complex on T8ML-1. Gene-modified T8ML-1 subclones with different expression levels of cell-surface TCR-α/β/CD3 complex were prepared: T8ML-1.1, in which TCR-α/β and CD3 were totally silenced; T8ML-1.1v, in which TCR-α/β and CD3 were partially knocked down; and T8ML-1.2, in which endogenous TCR was replaced with full-length HLA-A*24:02-restricted $WT1_{235-243}$-specific TCR-α/β with full expression of both cell-surface TCR-α/β and CD3. Degree of TCR-α/β and CD3 expression of each effector was laid out over the corresponding cytotoxicity mediated by each effector. Lectin-dependent cytotoxicity was partially inhibited by T8ML-1.1v, totally abrogated by T8ML-1.1, and was restored by T8ML-1.2. Experiments were performed at various *E:T* ratios in triplicate. Data are shown as mean ± SD. *** less than detectable. **b** PHA-P ligation induces phosphorylation of the CD3ζ chain of T8ML-1. (1) Western blotting showed that phosphorylation of the CD3ζ chain was clearly evoked after PHA-P ligation in T8ML-1, but not in T8ML-1.1, and restored by T8ML-1.2, examined. Representative data from 3 experiments are shown. (2) OKT-3 (10 μg) also phosphorylated the CD3ζ chain of T8ML-1 similarly to normal $CD8^+$ T-lymphocytes. P-CD3ζ: phosphorylated CD3ζ chain

53% at a 20:1 *E:T* ratio, and was decreased to 13% for T8ML-1.1v, a bulk line of T8ML-1 in which endogenous TCR expression had been partially knocked down (33.7% positive for TCR-α/β, and 33.1% positive for CD3). Eventually, this cytotoxicity was totally abrogated by T8ML-1.1 in which endogenous TCR-α/β and CD3

expression was absent. Additionally, this lectin-dependent cytotoxicity against Jurkat (40% at a 20:1 *E*:*T* ratio) was restored by T8ML-1.2 in which endogenous TCR was replaced with WT1-specific TCR. T8ML-1.2 also fully restored the surface expression of both TCR-α/β (99.4%) and CD3 (99.5%). We then examined whether or not PHA-P ligation delivered the TCR/CD3 complex-activating signal. As shown in Fig. 3b(1), PHA-P ligation strongly induced phosphorylation of the CD3ζ chain in T8ML-1, but not in T8ML-1.1, and this phosphorylation of the CD3ζ chain was also apparently restored in T8ML-1.2. As a control, OKT3 also induced phosphorylation of the CD3ζ chain in T8ML-1 as was that in normal $CD8^+$ T-lymphocytes in Fig. 3b(2). From these findings, we concluded that, PHA-P ligation to T8ML-1 activated the TCR/CD3 signaling pathway, subsequently triggering cytotoxic granular exocytosis, and eventually resulting in the lectin-dependent cytotoxicity.

3.4 Soluble factors produced by PHA-P treated T8ML-1 cells induced phagocytosis by human monocytes in the presence of surface expression of the TCR molecule

Next, we examined whether soluble factors produced by PHA-P-treated T8ML-1 cell were able to stimulate human monocytes to induce phagocytosis, as hemophagocytosis was a feature in the present patient. We found that the supernatant of PHA-P-treated T8ML-1, but not T8ML-1.1, increased the expressions of activation markers on human

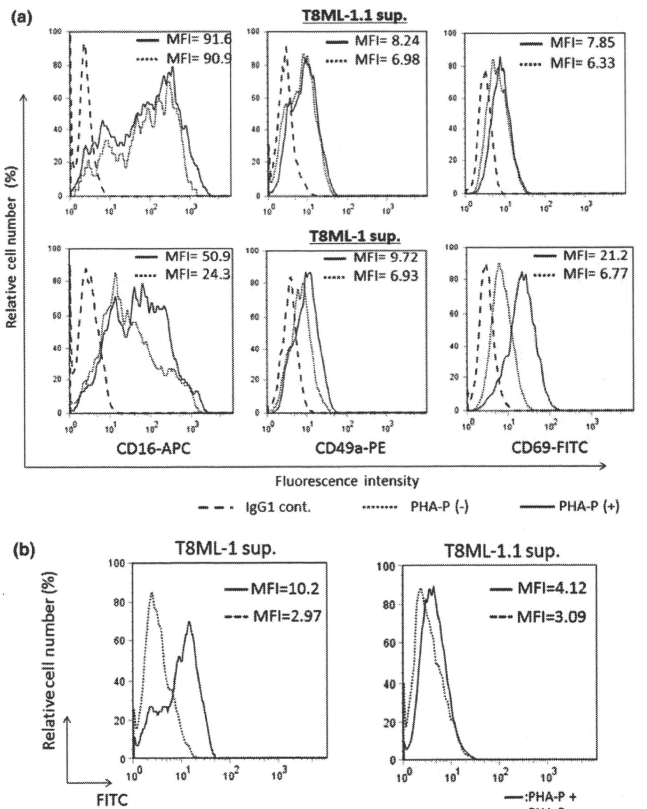

Fig. 4 **a** Activation of human monocytes by soluble factors produced by PHA-P-treated T8ML-1. Monocytes obtained from healthy volunteers were co-cultured with culture supernatant from T8ML-1 or T8ML-1.1 treated with PHA-P for 24 h. Expression of CD16, CD49a, and CD69, of monocytes was examined by flow cytometry. Culture supernatant of PHA-P-untreated T8ML-1 or T8ML-1.1 was used as a negative control. Compared with T8ML-1.1, the culture supernatant from PHA-P-treated T8ML-1 strongly augmented the activation status of monocytes. Representative data from 3 experiments are shown. *MFI* mean fluorescence intensity, *sup.* supernatant. **b** Soluble factors produced by PHA-P-treated T8ML-1, but not T8ML-1.1 activate phagocytosis by monocytes. Monocytes co-cultured in culture supernatant of PHA-P-treated T8ML-1, but not T8ML-1.1, were strongly activated to engulf the FITC-labeled latex beads (*solid line*). Culture supernatants of PHA-untreated T8ML-1 and T8ML-1.1 were prepared as a negative control, respectively. Both monocytes treated with supernatant of PHA-untreated T8ML-1 and T8ML-1.1 were negative for FITC (*dashed line*). Representative data from 3 experiments are shown. *MFI* mean fluorescence intensity, *sup.* supernatant

monocytes [10, 31]: MFI for CD16, CD49a and CD69 of each monocytes treated separately with supernatant from PHA-treated or untreated T8ML-1, or with that from T8ML-1.1 are shown in Fig. 4a. Representative data from three experiments using three individual samples are shown. Furthermore, phagocytosis assay revealed that the supernatant of PHA-P-treated T8ML-1, but not T8ML-1.1, stimulated human monocytes to engulf FITC-labeled latex beads. The proportion of FITC-positive monocytes was augmented by supernatant from PHA-P-treated T8ML-1 (FI = 2.43), but not that from PHA-P-treated T8ML-1.1 (FI = 0.33), in comparison to supernatant from PHA-P-untreated T8ML-1 (Fig. 4b). Thus, the TCR molecule on T8ML-1 was also essential for the production of these monocyte-mediated, phagocytosis-inducing soluble factors by PHA-P-treated T8ML-1.

3.5 Production of IFN-γ and TNF-α by PHA-P-treated T8ML-1 requires surface expression of the TCR molecule

Because IFN-γ and TNF-α have been reported to play a causative in LAHS [11–13], we examined the concentrations of both cytokines in supernatants of PHA-P-treated or untreated T8ML-1, T8ML-1.1, and T8ML-1.2 by ELISA. TNF-α production was significantly augmented by PHA in T8ML-1, but not in T8ML-1.1. Furthermore, TNF-α production was significantly restored by PHA-P-treated T8ML-1.2 with full expression of both cell-surface TCR and CD3 (Fig. 5a). Although T8ML-1 appeared to produce somewhat IFN-γ spontaneously, the significantly augmented IFN-γ production resulting from PHA-P-treatment was similarly dependent on the cell-surface expression of TCR (Fig. 5b). These results indicated that phagocytosis-inducible TNF-α and IFN-γ production by PHA-P-treated T8ML-1 also required cell-surface expression of the TCR molecule.

3.6 Soluble factors produced by PHA-P-treated-T8ML-1 activate human monocytes to engulf autologous RBC and PLT

Finally we examined whether soluble factors produced by PHA-P-treated T8ML-1 were able to induce hemophagocytosis. We co-cultured monocytes and RBC or PLT isolated from the same healthy individual with culture supernatant of PHA-P-treated or -untreated T8ML-1. Representative micrographs from three experiments were shown in Fig. 6. Only monocytes co-cultured with culture supernatant of PHA-P-treated T8ML-1 appeared to engulf the autologous RBC (Fig. 6b, c) and autologous PLT (Fig. 6e, f), whereas the same monocytes co-cultured with the culture supernatant of T8ML-1 without PHA-P did not

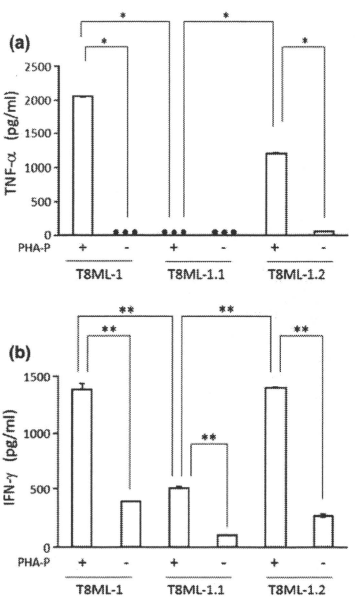

Fig. 5 Both PHA-P induced TNF-α and IFN-γ production by T8ML-1 requires cell-surface expression of the TCR molecule. **a** PHA-P treatment triggered the production of TNF-α by T8ML-1, which was totally abrogated by T8ML-1.1, and eventually was restored by T8ML-1.2. Data are shown as mean ± SD from 3 experiments. *p value < 0.001, ••• less than detectable. **b** Although T8ML-1and T8ML-1.2 spontaneously produced somewhat IFN-γ, PHA-P-treatment significantly augmented the production of IFN-γ by T8ML-1, which was significantly suppressed by T8ML-1.1, and restored by T8ML-1.2. Data are shown as mean ± SD from 3 experiments. **p value < 0.01

show such phagocytic activity (Fig. 6a, d, respectively). Additionally, the culture supernatant of PHA-P-treated T8ML-1.1 induced neither erythrophagocytosis nor thrombophagocytosis in this series of experiments (data not shown). These data confirmed that soluble factors produced by PHA-P-treated T8ML-1 were able to induce hemophagocytosis, and that this activity was dependent on the lymphoma cell TCR molecule.

4 Discussion

PTCL is an aggressive form of lymphoma that is often complicated by hemophagocytic syndrome (LAHS) that can adversely affect the clinical course of PTCL patients [8]. Proinflammatory cytokines play a significant role in

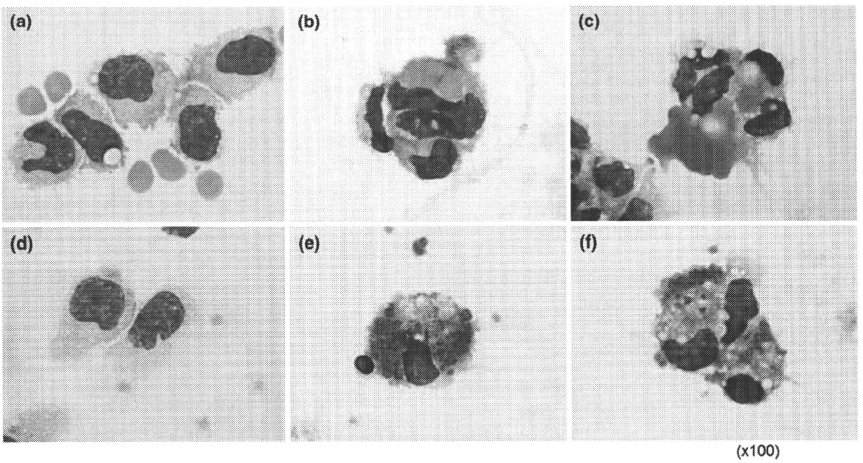

Fig. 6 Induction of erythrophagocytosis and thrombophagocytosis in activated monocytes by soluble factors derived from PHA-P-treated T8ML-1. Only the culture supernatant from PHA-P-treated T8ML-1 activated normal monocytes to exhibit erythrophagocytosis (**b** and **c**) and thrombophagocytosis (**e** and **f**), but neither (**a** and **d**, respectively) was evoked by supernatant from PHA-P-untreated T8ML-1. Experiments were independently performed with blood samples from 3 independent healthy volunteer', and representative data are shown

activating non-malignant macrophages to trigger LAHS in B-cell lymphoma and EBV-related PTCL. IFN-γ and TNF-α are representative, being overproduced by lymphoma cells [9, 11, 13], although details of the mechanism of LAHS in PTCL have not been fully clarified.

In the present study, by focusing on the TCR molecule expressed on lymphoma cells, we used non-antigen-specific T-cell stimulation with lectin [32] throughout the series of experiments. Finally, we addressed two possible mechanisms for the tissue-destructive manifestations clinically observed in this case using our newly established T8ML-1. First, we demonstrated the inducible, but not constitutive cytotoxicity mediated by T8ML-1 itself (Fig. 2a). T8ML-1 had an activated mature T-cell phenotype (Table 1) with redundant intracellular cytotoxic molecules (perforin and granzyme B) (Fig. 2c), and consequently exerted PHA-dependent cytotoxicity via cytotoxic granular exocytosis (Fig. 2b), and not via the Fas-Fas-L system. Activation of TCR downstream signaling was essential for this cytotoxic action of T8ML-1. Like OKT3 ligation, this PHA-induced cytotoxic granular exocytosis was initially routed through the phosphorylation of CD3ζ, one of the central signaling proteins of the TCR/CD3 complex [33–35]. This cytotoxic phenomenon was totally inhibited when the endogenous TCR was knocked out, and was restored by re-introduction of a new TCR with full cell-surface expression (Fig. 3a). Second, we demonstrated that soluble factors including TNF-α and IFN-γ, produced by PHA-treated T8ML-1, but not by normally cultured T8ML-1, appeared to activate erythrophagocytosis and thrombophagocytosis by human monocytes in vitro (Fig. 6a–f). Interestingly, this induction of hemophagocytosis by soluble factors released from PHA-treated T8ML-1, which were not constitutively produced by the T8ML-1, also required the activation of TCR signaling, because this phagocytosis-induction was totally abrogated by T8ML-1.1 (Fig. 4b). Collectively these findings strongly suggested that the TCR molecule on lymphoma cells might be essentially involved in clinical manifestations observed in the present case.

Regarding to the correlation between PTCL-LAHS and TCR expression on PTCL cells, it has been clinically observed that anaplastic large cell lymphoma (ALCL), a subtype of PTCL that is largely positive for CD4 but negative for CD8, CD3 and surface TCR-$\alpha\beta$ [36], tends to be complicated with LAHS less frequently than PTCL,NOS [8]. This seems to support our hypothesis that TCR on lymphoma cells plays an important role in the formation of PTCL-associated LAHS. Although, in this study, we could not determine the precise mechanism how TCR on lymphoma cells were activated, in vivo, we proposed a non-antigen specific activation model, such as with

lectins. Recently the important correlation between the survival of follicular lymphoma cells and in vivo lectins through lymphoma cell B-cell receptor stimulation has been reported [37], thus in vivo microenvironmental lectins might also activate PTCL cells through TCR stimulation. At the same time, lectins can also be provided in infectious conditions [32]. In this setting, normal $CD8^+$ T-lymphocytes can similarly be stimulated by lectins, however, contrary to T8ML-1, PHA-stimulated normal $CD8^+$ T-lymphocytes did not produce IFN-γ in vitro (data not shown), as has been already reported by other group [38]. Therefore, in such a condition of non-antigen-specific stimulation with lectins, PTCL cells may be more predominantly involved in exacerbating inflammatory milieu that can cause LAHS. Collectively, although we could not determine the precise activation mechanism of TCR on lymphoma cells in vivo, our observations suggest that the activation of TCR signaling in PTCL lymphoma cells might have a potentially important role in the formation of LAHS. However, further investigations are naturally warranted before our observations can be extrapolated to clinical cases.

Acknowledgments We are grateful for the skilled technical assistance of Ms. Junko Mizumoto and Dr. Kenji Kameda, Ehime University (Toon, Japan). We thank Dr. Hiroo Saji, HLA Laboratory, Japan, for HLA typing, and Dr. Shinichi Mizuno, Kurume University (Kurume, Japan), for the construction of lentiviral vector. This work was supported in part by grants from the Ministry of Education, Culture, Sports, Science and Technology of Japan, and Mitsubishi Pharma Research Foundation.

Conflict of interest All authors declare no conflict of interest.

References

1. Savage KJ. Peripheral T-cell lymphomas. Blood Rev. 2007;21:201–16.
2. Boulland ML, Kanavoros P, Wechsler J, Casiraghi O, Gaulard P. Cytotoxic protein expression in natural killer cell lymphomas and in $\alpha\beta$ and $\gamma\delta$ peripheral T-cell lymphomas. J Pathol. 1997; 183:432–9.
3. Mukai HY, Hasegawa Y, Kojima H, Okoshi Y, Takei N, Yamashita Y, et al. (2002) Nodal CD8 positive cytotoxic T-cell lymphoma: a distinct clinicopathological entity. Mod Pathol. 2002;15:1131–9.
4. Lee Y, Uhm JE, Lee HY, Park MJ, Kim H, Oh SJ, et al. Clinical features and prognostic factors of patients with "peripheral T cell lymphoma, unspecified". Ann Hematol. 2009;88:111–9.
5. Piccaluga PP, Agostinelli C, Califano A, Rossi M, Basso K, Zupo S, et al. Gene expression analysis of peripheral T cell lymphoma, unspecified, reveals distinct profiles and new potential therapeutic targets. J Clin Invest. 2007;117:823–34.
6. Falini B, Pileri S, De Solas I, Martelli MF, Mason DY, Delsol G, et al. Peripheral T-cell lymphoma associated with hemophagocytic syndrome. Blood. 1990;75:434–44.
7. Tong H, Ren Y, Liu H, Xiao F, Mai W, Meng H, et al. Clinical characteristics of T-cell lymphoma associated with hemophagocytic syndrome: comparison of T-cell lymphoma with and without hemophagocytic syndrome. Leuk Lymphoma. 2008;49:81–7.
8. Tong H, Ren Y, Qian W, Xiao F, Mai W, Meng H, et al. Clinicopathological study on peripheral T-cell non-Hodgkin lymphoma with bone marrow involvement: a retrospective analysis from China. Int J Hematol. 2009;90:303–10.
9. Al-Hashmi I, Decoteau J, Gruss HJ, Zielenska M, Thorner P, Poon A, et al. Establishment of a cytokine-producing anaplastic large-cell lymphoma cell line containing the t(2;5) translocation: potential role of cytokines in clinical manifestations. Leuk Lymphoma. 2001;40:599–611.
10. Takeyama N, Yabuki T, Kumagai T, Takagi S, Takemoto S, Noguchi H. Selective expansion of the CD14+/CD16 bright subpopulation of circulatory monocytes in patients with hemophagocytic syndrome. Ann Hematol. 2007;86:787–92.
11. Ohno T, Ueda Y, Nagai K, Takahashi T, Konaka Y, Takamatsu T, et al. The serum cytokine profile of lymphoma-associated hemophagocytic syndrome: a comparative analysis of B-cell and T-cell/natural killer cell lymphoma. Int J Hematol. 2003; 77:286–93.
12. Chuang HC, Lay JD, Hsieh WC, Su IJ. Pathogenesis and mechanism of disease progression from hemophagocytic lymphohistiocytosis to Ebstein–Barr virus-associated T-cell lymphoma: nuclear factor-κB pathway as a potential therapeutic target. Cancer Sci. 2007;98:1281–7.
13. Chuang HC, Lay JD, Chuang SE, Hsieh WC, Chang Y, Su IJ. Epstein-Barr virus (EBV) latent membrane protein-1 down-regulates tumor necrosis factor-alpha (TNF-alpha) receptor-1 and confers resistance to TNF-alpha-induced apoptosis in T cells: implication for the progression to T-cell lymphoma in EBV-associated hemophagocytic syndrome. Am J Pathol. 2007; 170:1607–17.
14. Jones D. Functional classification of peripheral T-cell lymphomas as an approach to improve outcome prediction and therapy selection. Semin Hematol. 2010;47(Suppl 1):S1–4.
15. Herling M, Patel KA, Teitell MA, Konopleva M, Ravandi F, Kobayashi R, et al. High TCL1 expression and intact T-cell receptor signaling defines a hyperproliferative subset of T-cell prolymphocytic leukemia. Blood. 2008;111:328–37.
16. Ansell SM, Habemann TM, Kurtin PJ, Witzig TE, Chen MG, Li CY, et al. Predictive capacity of the international prognostic factor index in patients with peripheral T-cell lymphoma. J Clin Oncol. 1997;15:2296–301.
17. Vose J, Armitage J, Weisenburger D. International peripheral T-cell and natural killer/T-cell lymphoma study: pathology findings and clinical outcome. J Clin Oncol. 2008;26:4124–30.
18. Iqbal J, Weisenburger DD, Greiner TC, Vose JM, McKeithan T, Kucuk C, et al. Molecular signatures to improve diagnosis in peripheral T-cell lymphoma and prognostification in angioimmunoblastic T-cell lymphoma. Blood. 2010;115:1026–36.
19. Gallamini A, Stelitano C, Calvi R, Bellei M, Mattei D, Vitolo U, et al. Peripheral T-cell lymphoma unspecified (PTCL-U): a new prognostic model from a retrospective multicentric clinical study. Blood. 2004;103:2474–9.
20. Wozniak MB, Villuendas R, Bischoff JR, Aparicio CB, Martinez Leal JF, de La Cueva P, et al. Vorinostat interferes with the signal transduction pathway of T-cell receptor and synergizes with phosphoinositide-3 kinase inhibitors in cutaneous T-cell lymphoma. Haematologica. 2010;95:613–21.
21. Costello R, Sanchez C, Le Treut T, Rihet P, Imbert J, Sebahoun G. Peripheral T-cell lymphoma gene expression profiling and potential therapeutic exploitations. Br J Haematol. 2010; 150:21–7.
22. Pechloff K, Holch J, Ferch U, Schweneker M, Brunner K, Kremer M, et al. The fusion kinase ITK-SYK mimics a T cell receptor

signal and drives oncogenesis in conditional mouse models of peripheral T cell lymphoma. J Exp Med. 2010;207:1031–44.
23. Rauch D, Gross S, Harding J, Bokhari S, Niewiesk S, Lairmore M, et al. T-cell activation promotes tumorigenesis in inflammation-associated cancer. Retrovirology. 2009;6:116.
24. Akatsuka Y, Martin EG, Madonik A, Barsoukov AA, Hansen JA. Rapid screening of T-cell receptor (TCR) variable gene usage by multiplex PCR: Application for assessment of clonal composition. Tissue Antigens. 1999;53:122–34.
25. Giudicelli V, Duroux P, Ginestoux C, Folch G, Jabado-Michaloud J, Chaume D, et al. IMGT/LIGM-DB, the IMGT comprehensive database of immunoglobulin and T cell receptor nucleotide sequences. Nucleic Acids Res. 2006;34(Database issue):D781–4.
26. Okamoto S, Mineno J, Ikeda H, Fujiwara H, Yasukawa M, Shiku H, et al. Improved expression and reactivity of transduced tumor-specific TCRs in human lymphocytes by specific silencing of endogenous TCR. Cancer Res. 2009;69:9003–11.
27. Ohminami H, Yasukawa M, Fujita S. HLA-class I-restricted lysis of leukemia cells by a CD8+ cytotoxic T-lymphocyte specific for WT1 peptide. Blood. 2000;95:286–93.
28. Yasukawa M, Inatsuki A, Horiuchi T, Kobayashi Y. Functional heterogeneity among herpes simplex virus-specific human $CD4^+$ T cells. J Immunol. 1991;146:1341–7.
29. Yasukawa M, Ohminami H, Arai J, Kasahara Y, Ishida Y, Fujita S. Granule exocytosis, and not the fas/fas ligand system, is the main pathway of cytotoxicity mediated by alloantigen-specific $CD4^+$ as well as $CD8^+$ cytotoxic T lymphocytes in humans. Blood. 2000;95:2352–5.
30. Ochi T, Fujiwara H, Suemori K, Azuma T, Yakushijin Y, Hato T, et al. Aurora-A kinase: a novel target of cellular immunotherapy for leukemia. Blood. 2009;113:66–74.
31. Heron M, Grutters JC, van Velzen-Blad H, Veltkamp M, Claessen AM, van den Bosch JM. Increased expression of CD16, CD69, and very late antigen-1 on blood monocytes in active sarcoidosis. Chest. 2008;134:1001–8.
32. Green WR, Ballas ZK, Henney CS. Studies on the mechanism of lymphocyte-mediated cytolysis: XI. The role of lectin in lectin-dependent cell-mediated cytotoxicity. J Immunol. 1987;121:1566–72.
33. Radoja S, Frey AB, Vukmanovic S. T-cell receptor signaling events triggering granular exocytosis. Crit Rev Immunol. 2006;26:265–90.
34. Ma JS, Haydar TF, Radoja S. Protein kinase C δ localizes to secretory lysozomes in $CD8^+$ CTL and directly mediates TCR signals leading to granule exocytosis-mediated cytotoxicity. J Immunol. 2008;181:4716–22.
35. Sitkovsky MV. Mechanistic, functional and immunopharmacological implications of biochemical studies of antigen receptor-triggered cytolytic T-lymphocyte activation. Immunol Rev. 1988;103:127–60.
36. Geissinger E, Sadler P, Roth S, Grieb T, Puppe B, et al. Disturbed expression of the T-cell receptor/CD3 complex and associated signaling molecules in $CD30^+$ T-cell lymphoproliferations. Haematologica. 2010;95:1697–704.
37. Coelho V, Krysov S, Ghaemmaghami AM, Emara M, Potter KN, Johnson P, et al. Glycosylation of surface Ig creates a functional bridge between human follicular lymphoma and microenvironmental lectins. Proc Natl Acad Sci USA. 2010. doi:10.1073/pnas.1009388107 (early edition).
38. Branchiley JM, Douek DC, Ambrozak DR, Chatterji M, Betts MR, Davis LS, et al. Expansion of activated human naïve T-cells precedes effector function. Clin Exp Immunol. 2002;130:431–40.

The Human Cytomegalovirus UL76 Gene Regulates the Level of Expression of the UL77 Gene

Hiroki Isomura[1]*, Mark F. Stinski[3], Takayuki Murata[1], Sanae Nakayama[1], Shigeki Chiba[1], Yoshiki Akatsuka[2], Teru Kanda[1], Tatsuya Tsurumi[1]

1 Division of Virology, Aichi Cancer Center Research Institute, Kanokoden, Nagoya, Japan, **2** Division of Immunology, Aichi Cancer Center Research Institute, Kanokoden, Nagoya, Japan, **3** Department of Microbiology, Carver College of Medicine, University of Iowa, Iowa City, Iowa, United States of America

Abstract

Background: Human cytomegalovirus (HCMV) can be reactivated under immunosuppressive conditions causing several fatal pneumonitis, hepatitis, retinitis, and gastrointestinal diseases. HCMV also causes deafness and mental retardation in neonates when primary infection has occurred during pregnancy. In the genome of HCMV at least 194 known open reading frames (ORFs) have been predicted, and approximately one-quarter, or 41 ORFs, are required for viral replication in cell culture. In contrast, the majority of the predicted ORFs are nonessential for viral replication in cell culture. However, it is also possible that these ORFs are required for the efficient viral replication in the host. The UL77 gene of HCMV is essential for viral replication and has a role in viral DNA packaging. The function of the upstream UL76 gene in the HCMV-infected cells is not understood. UL76 and UL77 are cistons on the same viral mRNA and a conventional 5′ mRNA for UL77 has not been detected. The vast majority of eukaryotic mRNAs are monocistronic, i.e., they encode only a single protein.

Methodology/Principal Findings: To determine whether the UL76 ORF affects UL77 gene expression, we mutated UL76 by ORF frame-shifts, stop codons or deletion of the viral gene. The effect on UL77 protein expression was determined by either transfection of expression plasmids or infection with recombinant viruses. Mutation of UL76 ORF significantly increased the level of UL77 protein expression. However, deletion of UL76 upstream of the UL77 ORF had only marginal effects on viral growth.

Conclusions/Significance: While UL76 is not essential for viral replication, the UL76 ORF is involved in regulation of the level of UL77 protein expression in a manner dependent on the translation re-initiation. UL76 may fine-tune the UL77 expression for the efficient viral replication in the HCMV- infected cells.

Citation: Isomura H, Stinski MF, Murata T, Nakayama S, Chiba S, et al. (2010) The Human Cytomegalovirus UL76 Gene Regulates the Level of Expression of the UL77 Gene. PLoS ONE 5(7): e11901. doi:10.1371/journal.pone.0011901

Editor: Robyn Klein, Washington University, United States of America

Received March 18, 2010; **Accepted** July 7, 2010; **Published** July 30, 2010

Funding: This work was supported by Grants-in-aid for Scientific Research on Priority Areas from the Ministry of Education, Science, Sports, Culture and Technology of Japan (20012056, 19041078, 20390137 to T.T., and 19590487 to H.I.), Research on Health Sciences focusing on Drug Innovation (SH54412 to H.I.), a Grant-in-aid for Cancer Research (19-01 to H.I.) from the Ministry of Health, Labor and Welfare, and grant AI-13562 from the National Institutes of Health (to M.F.S.). The funders had no role in study design, data collection and analysis, decision to publish, or preparation of the manuscript.

Competing Interests: The authors have declared that no competing interests exist.

* E-mail: hisomura@aichi-cc.jp

Introduction

Human cytomegalovirus (HCMV) is the prototype member of the betaherpesvirus family. Although infection by HCMV occurs in most individuals, it is usually asymptomatic. The virus can be reactivated under immunosuppressive conditions to become a pathogen that causes pneumonitis, hepatitis, retinitis, and gastrointestinal diseases. HCMV also causes deafness and mental retardation in neonates when primary infection has occurred during pregnancy.

The genome of HCMV is approximately 240,000 base pairs (bps) in size, and at least 194 known open reading frames (ORFs) are predicted [1,2,3]. Global mutational analyses of the viral ORF by constructing virus gene-deletion mutants indicates that approximately one-quarter, or 41 ORFs, are required for viral replication in cell culture [4]. The majority of the ORFs are nonessential for viral replication in cell culture. Several ORFs are beneficial but not required for viral replication.

During productive infection, HCMV genes are expressed in a temporal cascade, designated immediate early (IE), delayed early, and late. The major IE genes (MIE) UL123/122 (IE1/IE2) play a critical role in subsequent viral gene expression and the efficiency of viral replication [5,6,7,8,9,10]. The early viral genes encode proteins necessary for viral DNA replication [11]. Following viral DNA replication, delayed early and late viral genes are expressed which encode structural proteins for viral production.

Global mutational analysis by constructing virus gene-deletion mutants classified UL77 as essential and UL76 as essential [1] or augmenting [4] for viral replication. The human cytomegalovirus (HCMV) UL76 and UL77 genes have open reading frames (ORFs) that partially overlap on the same viral transcript, but UL77 is in a different ORF. An mRNA with a 5′ end upstream of UL77 has not been detected [12]. Viral mRNAs with two or more ORFs downstream of the 5′ end is a feature frequently encountered among the HCMV transcripts [13,14,15,16,17,18,19]. However,

the effect of the upstream ORF on the downstream ORF expression and on viral replication is not understood. We determined the effect of the UL76 ORF on UL77 gene expression and viral replication.

The UL76 gene encodes a highly conserved virion-associated herpesvirus protein of 38 kDa, which is detected in HCMV-infected cells at 2 h post-infection (p.i.). Production of the viral protein reaches a maximum at 24 h p.i. and then the level remains the same through the late phase of the virus life-cycle [12,20]. The UL77 protein, which is the counterpart of the herpes simplex virus (HSV) UL25 DNA packaging protein, is essential for HCMV replication [1,4].

In the present study, we report that UL76 sequence is involved in the regulation of the UL77 gene expression in a manner dependent on the translation reinitiation. Since UL77 is essential for viral replication, understanding how UL77 gene expression is controlled is important. UL76 sequence may fine-tune the level of the UL77 expression for the efficient viral replication in the HCMV- infected cells.

Results

Deletion of the region upstream of UL77

To confirm that there is not a transcription start site for UL77 within the UL76 ORF, we constructed a recombinant virus in which the UL76 gene was deleted. Since a drug resistant gene is necessary to select the recombinant BAC DNA from wt, we constructed the recombinant BAC DNAs to contain the kanamycin resistant gene (KanR). To avoid the possibility that KanR would affect expression of the neighboring gene, we constructed recombinant BAC DNAs with FRT sequence flanking. KanR was excised by FLP-mediated recombination. After excision of the KanR, only 34 bp of FRT was left in front of the UL77 ORF (Fig. 1a). Since the UL76 ORF contains a BstB I site (Fig. 1a), BAC DNAs were digested with the restriction endonuclease BstB I. Viral DNA fragments were fractionated by electrophoresis in 0.6% agarose gels, and immobilized for Southern blot hybridization with probes for either UL75 or UL76 as described in the Materials and Methods. With the UL75 probe, a larger viral DNA fragment was detected when UL76 was deleted (Fig. 1b, left panel). The DNA fragment containing UL76 was not detected with the UL76 probe for recombinant virus RdlUL76+F, whereas, it was detected for the wild type (Fig. 1b, right panel). PCR analysis revealed the recombination in the recombinant BAC DNA (data not shown). DNA sequencing confirmed the recombination (data not shown).

After viral isolation, cells were infected at an MOI of 1 and assayed for the UL76, UL77 and UL78 transcripts by Northern blotting at 6, 24, 48, and 72 h.p.i. The high MOI was used in order to detect all viral RNAs from the UL77 region of the viral genome. Twenty microgram aliquots of RNA were subjected to agarose gel electrophoresis. Ethidium bromide staining of 28S and 18S ribosomal RNA confirmed that equal amounts of RNA were loaded in each lane (Fig. 1c and e). As expected, there was no transcript when UL76 was deleted for recombinant virus RdlUL76+F, but the transcript was detected for the wt (Fig. 1 c). There were no additional transcripts detected in the wt or Rdl76+F with the UL 77 probe (Fig. 1d). There was a transcript detected solely for the UL78 gene in the wt and recombinant virus RdlUL76+F with the UL78 probe (Fig. 1e). These results indicate that the UL77 ORF lacked the UL76 upstream region in RdlUL76+F.

UL76 ORF translation down-regulates UL77 expression

The vast majority of eukaryotic mRNAs are monocistronic, i.e., they encode only a single protein. To determine the effect of UL76 on UL77 expression, we constructed a plasmid with a flag epitope fused to the N- terminus of the UL76 ORF and a HA epitope fused to the C-terminus of the UL 77 ORF. We also constructed a plasmid with a frame shift mutation inserted into the N-terminus of the UL76 ORF or the C-terminus of the UL77 ORF (Fig. 2a). After transfection of HeLa cells, RT-PCR analysis showed that there was little difference in the amount of the UL77 transcripts between flagUL76-77HA and flagUL76-77-frame-shift-HA (Fig. 2b). The amount of UL77 RNA was reduced slightly (1.4-fold) with flag-frame-shift-UL76-77HA. This level of viral RNA decrease was considered marginal. After 48 h, equal amounts of protein were fractionated by 12.5% SDS-polyacrylamide gel electrophoresis (PAGE) and analyzed by Western blotting with a monoclonal antibody against a flag or HA epitope as described in the Materials and Methods. As shown in figure 2c, lane 2, both the UL76 and UL77 fusion proteins were expressed in HeLa cells transfected with pCMVflagUL76-77HA. However, when a frame-shift was inserted downstream of the ATG of the UL76 ORF, the level of expression of the UL77 fusion protein was increased approximately 4- fold (Fig. 2c, compare lanes 1 and 2).

To confirm the inhibitory effect of the UL76 ORF translation on the UL77 gene expression, we constructed plasmids with the luciferase gene fused to the C-terminus of the UL 77 ORF and inserted stop codons in the UL76 ORF at 13, 180 and 226 amino acid residues or introduced a frame-shift at 2 amino acid residues, the same as pCMVflag-frame-shift-UL76-77A (Fig. 3a). pCMV-Rluc served as a control for transfection efficiency. At 48 h post transfection, equal amounts of protein were fractionated by SDS-PAGE and analyzed by Western blotting with a monoclonal antibody against a flag epitope as described in the Materials and Methods. As shown in figure 3b, the wild type and the truncated forms of the UL76 protein were detected in cells transfected with the wild type, stop3, and stop4 plasmids (Lanes, 1, 3, and 4). Expression of the truncated forms of UL76 protein was not detected in cells transfected with stop1 or the frame-shift by 5–20% gradient SDS-PAGE (Fig. 3c). Since the frame-shift has the 80 amino acids of protein coding sequence from the start codon, why this protein was not detected by Western blotting is unclear. The protein translated from the artificial gene might be unstable. Real-time RT-PCR analysis indicated that there was not a significant difference in the amount of UL77 transcripts (Fig. 3d). After 48 h, equal amounts of protein were fractionated by 10% PAGE and analyzed by Western blotting with a monoclonal antibody against a luciferase protein as described in the Materials and Methods. As shown in figure 3e, when a stop codon was inserted at 13 amino acids downstream from the UL76 start codon, the level of expression of the UL77 fusion protein was increased approximately 4- fold compared to the wt (compare lanes, 1 and 2). Cell extracts were also assayed for luciferase activities 48 h after transfection. Stop 1 caused an approximately 4- fold increase in the luciferase activity ($p<0.0001$) (Fig. 3f). Insertion of a stop codon at 180 or 226 amino acids or a frame-shift at 2 amino acids caused an approximately 2- fold increase in the luciferase activity ($p<0.0001$, $p=0.0002$, or $p=0.05$, respectively) (Fig. 3f). From these results, we conclude that UL76 ORF translation significantly down- regulates the expression of the UL77 gene.

UL76 ORF translation affects the expression of the UL77 gene in the HCMV- infected cells

To determine whether insertion of a stop codon downstream of the ATG start codon for the UL76 ORF also affects UL77 gene expression in the HCMV- infected cells, we constructed a recombinant HCMV BAC DNA with a flag epitope fused to the

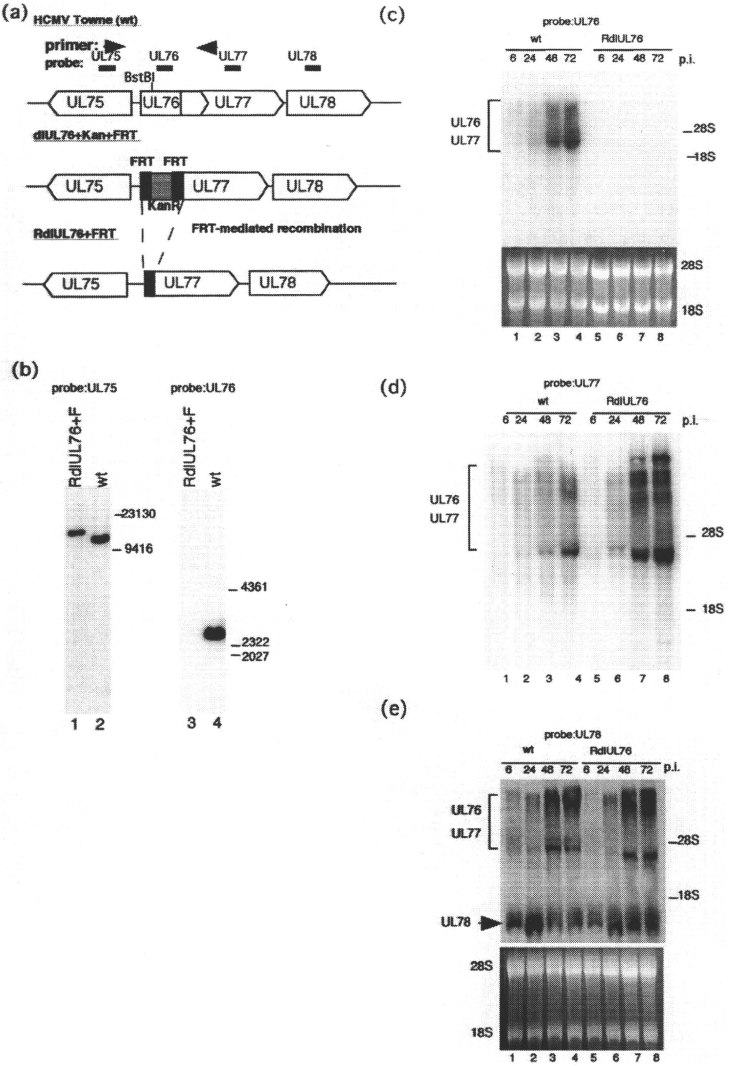

Figure 1. Analysis of UL76 to UL78 gene transcripts after infection with the wt and recombinant virus. (a) Diagram of the recombinant BAC DNAs of wt and RdlUL76+F. UL76 was replaced with the kanamycin resistant gene (KanR), and then KanR was excised by FLP-mediated recombination, leaving only 34 bp of the FRT sequence (F). (b) Southern blot analysis of parental and recombinant BAC-DNAs of wt and RdlUL76+F. BAC DNAs were digested with restriction endonuclease BstB I, fractionated by electrophoresis in 0.6% agarose, and subjected to hybridization with a ^{32}P-labeled probe. Standard molecular size markers are indicated in base pairs. Lanes: 1 and 3, RdlUL76+F; 2 and 4, wt; 1 and 2, UL75 probe; 3 and 4, UL76 probe. (c, d, and e) Analysis of UL76 to 78 gene transcripts after infection with the wt or RdlUL76+F. HFFs were infected with an MOI of 1, and

cytoplasmic RNA was harvested 6, 24, 48, and 72 h. p.i. as described in the Materials and Methods. 28S and 18S rRNA served as controls for equal amounts of RNA loading. (c), UL76 probe; (d), UL77 probe; (e), UL78 probe. Lanes: 1 and 5, 6 h.p.i.; 2 and 6, 24 h.p.i.; 3 and 7, 48 h.p.i.; 4 and 8, 72 h.p.i.; 1 to 4, wt; 5 to 8, RdlUL76+F.
doi:10.1371/journal.pone.0011901.g001

N- terminus of the UL77 ORF by reverse selection (Fig. 4). We also inserted the TAG stop codon downstream of the ATG start codon for the UL76 ORF as described in the Materials and Methods (Fig. 4, right panel). Lastly, we constructed a revertant BAC DNA (UL76revertantflagUL77) (Fig. 4, right panel). The integrity of the mutant BACs were checked by digestion with Hind III (data not shown) and the correct recombination was confirmed by sequencing of the PCR product (data not shown).

Cells were infected with either RUL76stopflagUL77 (RUL76-stop) or RUL76revertantflagUL77 (RUL76 rev.) at an MOI of 1,

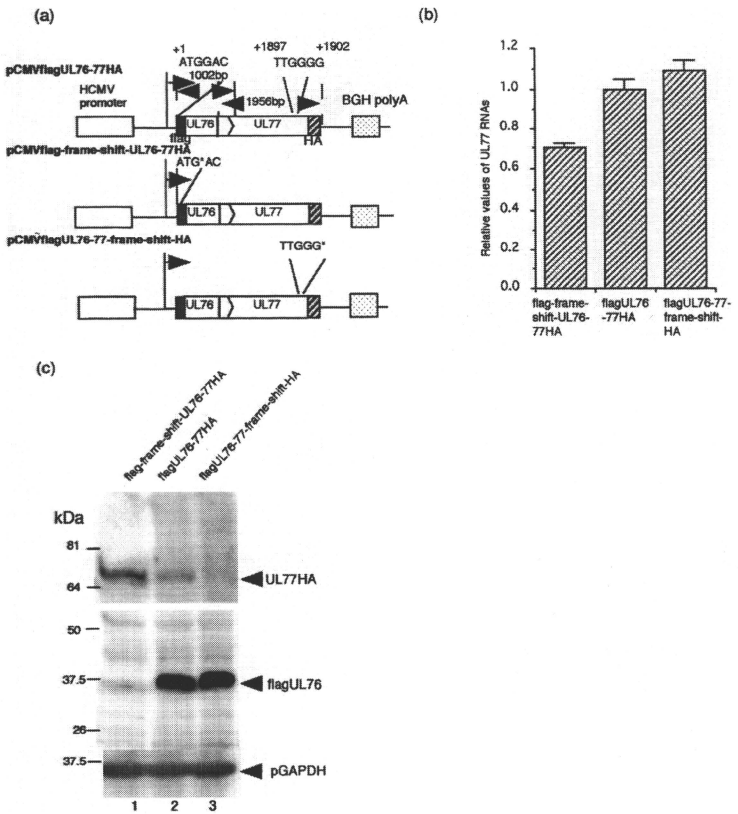

Figure 2. Expression plasmids with the UL76-77 sequence. (a) Diagram of expression plasmids with the UL76-77 sequence inserted downstream of the HCMV MIE promoter with or without frame-shifts. (b) Quantity of the UL77 gene transcripts with the expression plasmids. RNAs were analyzed with UL77 specific primers and probe by real-time PCR as described in the Materials and Methods. The assay was performed in triplicate, and the standard error of the mean was determined. RNAs were normalized to G6PD RNA, and each value was relative to the level of pCMVflagUL76-77HA. (c) Western blot analysis of UL76 and UL77 fusion proteins. HeLa cells were transfected with pCMVflagUL76-77HA with or without a frame shift mutation and harvested at 48 h post transfection. To detect the fusion protein with a flag or HA epitope, antibody F3165 (Sigma) or 3F10 (Roche) was used, respectively. Lanes: 1, pCMVflag-frame-shift-UL76-77HA; 2, pCMVflagUL76-77HA; 3, pCMVflagUL76-77-frame-shift-HA.
doi:10.1371/journal.pone.0011901.g002